Ohmic contacts to *p*-type GaN mediated by polarization fields in thin $In_xGa_{1-x}N$ capping layers

T. Gessmann,[a] Y.-L. Li, E. L. Waldron,[b] J. W. Graff, and E. F. Schubert
Department of Electrical and Computer Engineering, Boston University, Boston, Massachusetts 02215

J. K. Sheu
Optical Science Center, National Central University, Chung-Li 32054, Taiwan, Republic of China

(Received 27 September 2001; accepted for publication 26 November 2001)

Low-resistance ohmic contacts are demonstrated using thin *p*-type InGaN layers on *p*-type GaN. It is shown that the tunneling barrier width is drastically reduced by polarization-induced electric fields in the strained InGaN capping layers resulting in an increase of the hole tunneling probability through the barrier and a significant decrease of the specific contact resistance. The specific contact resistance of Ni (10 nm)/Au (30 nm) contacts deposited on the InGaN capping layers was determined by the transmission line method. Specific contact resistances of $1.2\times10^{-2}\ \Omega\,cm^2$ and $6\times10^{-3}\ \Omega\,cm^2$ were obtained for capping layer thicknesses of 20 nm and 2 nm, respectively. [DOI: 10.1063/1.1445807]

The performance of devices fabricated from GaN and related compounds is strongly affected by the resistances caused by electrical contacts. To avoid excessive heating resulting in failure of the device, specific contact resistances in the order of $<10^{-3}\ \Omega\,cm^2$ for light-emitting diodes (LEDs) and $<10^{-4}\ \Omega\,cm^2$ for laser diodes are required.[1] This applies in particular to ohmic contacts on *p*-type GaN (*p*-GaN) due to the resistive nature of GaN obtained by standard *p*-type doping techniques.[1,2]

Several methods have been utilized to attain low specific contact resistances to *p*-GaN such as deposition of high work function metals,[3] growth of AlGaN/GaN superlattices[4,5] and tunnel-diode structures on top of *p*-GaN.[6]

In this publication, the use of thin $In_xGa_{1-x}N$ capping layers pseudomorphically grown on top of *p*-type GaN is presented. Strain-induced piezoelectric as well as spontaneous polarization fields in the InGaN capping layer and the lower *p*-GaN layer cause band bending that leads to the formation of a two-dimensional hole gas (2DHG).[7] As a result, the concentration of free holes near the surface is greatly increased and the tunneling barrier width of the metal—semiconductor contact is reduced, thereby allowing for a high hole tunneling probability through the barrier. The theory describing *p*-type ohmic contacts to *p*-GaN by using thin $In_xGa_{1-x}N$ capping layers will be presented together with experimental results demonstrating the capability of the approach in achieving low contact resistances.

The samples were grown by metalorganic chemical vapor deposition along the *c* direction on top of single crystalline sapphire substrates. The grown structures consist of a 4 μm thick *n*-type GaN layer, a five pair multiquantum well LED with barrier/well widths of 7.5 nm/2.5 nm, respectively, a 20 nm $Al_{0.15}Ga_{0.85}N$ electron blocking layer, a 130 nm thick *p*-type GaN upper cladding layer and a *p*-type $In_{0.27}Ga_{0.73}N$ capping layer that is either 2 or 20 nm thick. The two *p*-type layers were Mg doped to a concentration of about $N_{Mg}=3\times10^{18}\ cm^{-3}$ as determined from capacitance–voltage measurements.

Ni(10 nm)/Au (30 nm) contacts were deposited by electron-beam evaporation using lift-off photolithographic techniques. The contacts were square-shaped pads (180 μm $\times$180 μm) separated by 2, 4, 6, 8, 10, and 15 μm wide gaps between the pads. To remove surface oxide layers the samples were dipped in a buffered-oxide etch solution for 3 min prior to mounting them in the deposition chamber. Subsequently, the contacts were annealed for 3 min in a rapid thermal annealing furnace at 500 °C in an oxygen atmosphere. The contact resistances were determined from current–voltage ($I-V$) measurements using the transmission-line method (TLM).

Figure 1 shows the band diagram of an elastically strained, 20 nm thick *p*-type $In_{0.27}Ga_{0.73}N$ capping layer on top of relaxed *p*-GaN, self consistently calculated by solving the coupled Schroedinger Poisson equations in one dimension.[8] We used a uniform Mg dopant concentration of

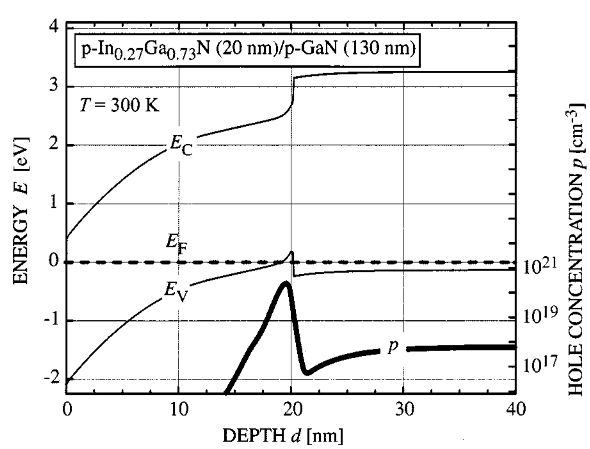

FIG. 1. Self-consistently calculated band diagram and free hole concentration *p* of a 20 nm thick *p*-type $In_{0.27}Ga_{0.73}N$ layer grown pseudomorphically on *p*-type GaN with a dopant concentration of $10^{19}\ cm^{-3}$.

[a]Electronic mail: gessmann@bu.edu
[b]Also at: Department of Physics, Boston University, Boston, Massachusetts 02215.

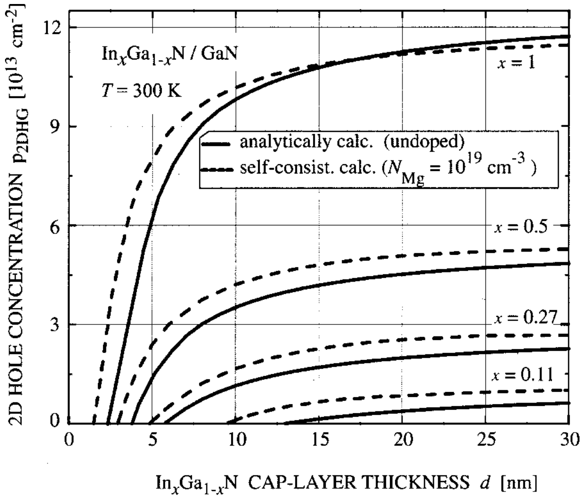

FIG. 2. Dependence of the 2DHG density, p_{2DHG}, on the InGaN capping layer thickness d for different indium contents x of the capping layer. The dashed curves correspond to the area of the peak in the self-consistently calculated depth distribution of the hole concentration p (see Fig. 1), the solid lines are numerical solutions of Eq. (1).

$N_{Mg} = 10^{19}$ cm^3. Also included in Fig. 1 is the calculated depth dependence of the hole concentration p.

It is evident that the strong band bending in the $In_{0.27}Ga_{0.73}N$ capping layer induced by the polarization fields results in a peak of the hole distribution close to the InGaN/GaN interface indicating the formation of a 2DHG. The band bending reduces the width of the tunneling barrier which can be estimated as the barrier thickness d^* at half the Schottky barrier height. From Fig. 1, we find $d^* \sim 5$ nm. This compares favorably to a calculated value of about 10 nm obtained for a p-type GaN structure without any capping layer.

Figure 2 shows the 2DHG density, p_{2DHG}, as a function of the thickness, d, and the In content, x, of the InGaN capping layer. The values for p_{2DHG} have been calculated either by integrating the peak area of the hole concentration p in Fig. 1 or by numerically solving the equation of energy conservation for a hole moving in the c direction through the InGaN capping layer

$$e\Phi_B + e\mathbf{E}d_{\mathrm{InGaN}} + (E_0 - E_V) + (E_F - E_0) = 0. \quad (1)$$

In Eq. (1), e is the positive elementary charge, d_{InGaN} denotes the thickness of the capping layer, **E** is the vector of the total electric field in the capping layer, Φ_B is the Schottky barrier height, E_V is the valence band energy; E_F and E_0 are the Fermi energy and the energy of the 2DHG groundstate, respectively. The different contributions to the left-hand side in Eq. (1) are given by

$$e\Phi_B = E_{G,\mathrm{InGaN}} - e(\Phi_M - \chi_{\mathrm{InGaN}}), \quad (2a)$$

$$\mathbf{E} = \mathbf{E}_{\mathrm{Sp,InGaN}} + \mathbf{E}_{\mathrm{Pz,InGaN}} - \mathbf{E}_{\mathrm{Sp,GaN}} + \frac{e p_{2DHG}}{\epsilon_{\mathrm{InGaN}}}, \quad (2b)$$

$$E_0 - E_V = \frac{3}{2}\left[\frac{3}{2}\frac{e^2\hbar}{\epsilon_{\mathrm{InGaN}}\sqrt{m^*}} p_{2DHG}\right]^{2/3}, \quad (2c)$$

$$E_F - E_0 = \frac{\pi\hbar^2}{m^*} p_{2DHG}. \quad (2d)$$

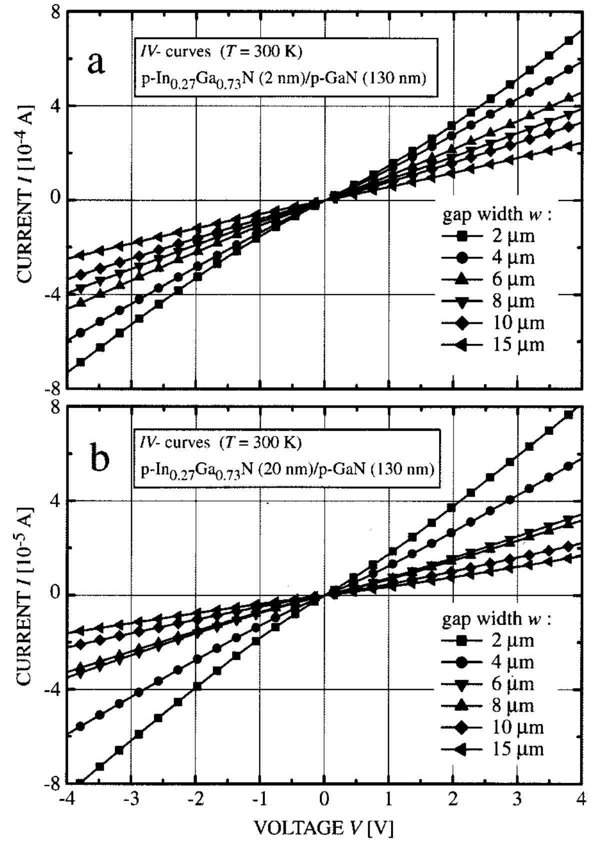

FIG. 3. $I-V$ curves measured on InGaN/GaN samples with a 2 nm thick (a) and a 20 nm thick (b) $In_{0.27}Ga_{0.73}N$ capping layer.

$E_{G,\mathrm{InGaN}}$ and χ_{InGaN} in Eq. (2a) are the band gap energy and the electron affinity of the $In_{0.27}Ga_{0.73}N$ capping layer, and Φ_M is the work function of the contact metal. The electron affinity χ_{InGaN} can be calculated from Anderson's rule[9] using a conduction band offset at the $In_{0.27}Ga_{0.73}N$/GaN interface according to $0.7\times(E_{G,\mathrm{GaN}} - E_{G,\mathrm{InGaN}})$. The subscripts "Sp" and "Pz" in Eq. (2b) correspond to the electric fields induced by the spontaneous and piezoelectric polarizations, $\epsilon_{\mathrm{InGaN}} = 10.4 + 3.9\times 0.27$ is the relative dielectric permeability of the $In_{0.27}Ga_{0.73}N$ capping layer.

In Eq. (2c), $E_0 - E_V$ was obtained using the Fang–Howard approximation[10] for energy states in a triangular well. The effective hole mass m^* is taken equal to the free electron mass m_0 and $\hbar$ is Planck's constant divided by 2π. $E_F - E_0$ in Eq. (2d) was calculated using the high-density approximation of the Fermi–Dirac distribution and the two-dimensional (2D) density of hole states $\rho_{2D} = m^*/(\pi\hbar^2)$. Comparison of the analytical results with the self-consistently calculated results shown in Fig. 2 reveals good agreement. Minor differences can be attributed to differences in doping concentration.

The $I-V$ characteristics of the contacts to both $In_{0.27}Ga_{0.73}N$ capping layers are linear for all the contact pad separations (see Fig. 3). However, at the same voltages, the current through the thick capping layer is about one order of magnitude smaller compared to the thin capping layer.

The pad-to-pad resistances calculated from the $I-V$ data for different pad separations are shown in Fig. 4 together with results of the TLM analysis of these data. The specific contact resistance $\rho_c = 6\times 10^{-3}$ Ω cm^2 for the 2 nm-capping

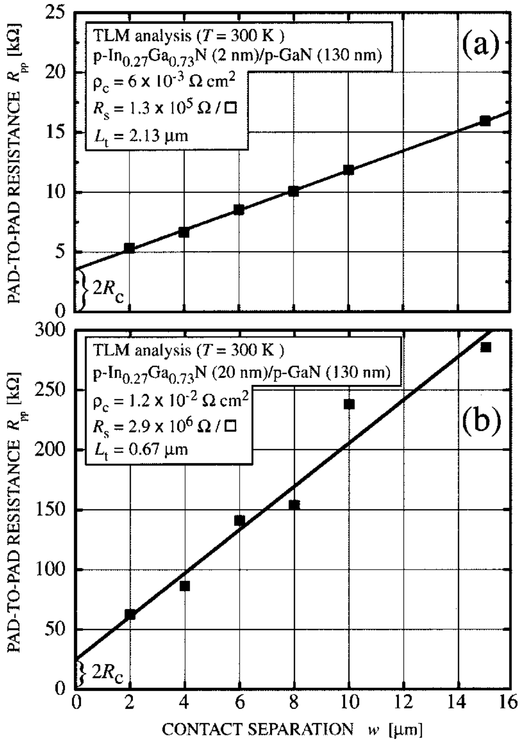

FIG. 4. Pad-to-pad resistances R_{pp} obtained from the $I-V$ curves in Fig. 3. The straight-line fits to the data (solid lines) are analyzed using the TLM model. The values obtained for the specific contact resistance ρ_c, the sheet resistance R_s and the transfer length L_t are shown in the insets.

layer is smaller by a factor of two than $\rho_c = 1.2 \times 10^{-2}\ \Omega\ \text{cm}^2$ for the 20 nm-layer. According to the Wentzel–Kramers–Brillouin approximation the one-dimensional hole tunneling probability T_z along the z direction through a semiconducting layer of width d can be written as

$$T_z = \exp\left[-\int_0^d 2\hbar^{-1}\sqrt{2m^* E_V(z)}\,dz\right]. \tag{3}$$

The tunneling probability T_z in Eq. (3) increases exponentially upon decreasing the layer thickness d. By reducing the thickness of the InGaN capping layer from 20 to 2 nm, however, the contact resistance changed only by a factor of 0.5; this might indicate limitations to the hole transport not taken into account by Eq. (3) possibly caused by defects such as dislocations in the InGaN capping layers or by approaching the critical thickness in the 20 nm thick capping layer.

In conclusion, we have shown a method utilizing the polarization in thin InGaN capping layers pseudomorphically grown on top of p-type GaN as a way to reduce the specific contact resistance. The $I-V$ curves of all contacts are strictly linear indicating excellent ohmicity of the contacts. Specific contact resistances of $\rho_c = 6 \times 10^{-3}\ \Omega\ \text{cm}^2$ and $\rho_c = 1.2 \times 10^{-2}\ \Omega\ \text{cm}^2$ have been obtained for capping layer thicknesses of 2 nm and 20 nm, respectively. These results are consistent with strong band bending in the capping layer region induced by polarization fields. As a result, the tunneling barrier width is reduced and the concentration of free holes increased. Further improvement of the specific contact resistance at least into the $10^{-5}\ \Omega\ \text{cm}^2$ range is expected by optimizing the thickness and surface morphology of the capping layer.

This work was supported by the Office of Naval Research and monitored by Dr. Colin E. C. Wood.

[1] S. J. Pearton, J. C. Zolper, R. J. Shul, and F. Ren, J. Appl. Phys. **86**, 1 (1999).
[2] O. Ambacher, J. Phys. D **31**, 2653 (1998).
[3] J. K. Ho, C.-S. Jong, C. C. Chiu, C.-N. Huang, K.-K. Shih, L.-C. Chen, F.-R. Chen, and J.-J. Kai, J. Appl. Phys. **86**, 4491 (1999).
[4] Y.-L. Li, E. F. Schubert, and J. W. Graff, Appl. Phys. Lett. **76**, 2728 (2000).
[5] J. K. Sheu, G. C. Chi, and M. J. Jou, IEEE Electron Device Lett. **22**, 160 (2001).
[6] S.-R. Jeon, Y.-H. Song, H.-J. Jang, G. M. Yang, S. W. Hwang, and S. J. Son, Appl. Phys. Lett. **78**, 3265 (2001).
[7] E. L. Waldron, J. W. Graff, and E. F. Schubert, Appl. Phys. Lett. **79**, 2737 (2001).
[8] We used the freeware program "1D Poisson/Schroedinger" available at http://www.nd.edu/~gsnider/.
[9] R. L. Anderson, Solid-State Electron. **5**, 341 (1962).
[10] F. F. Fang and W. E. Howard, Phys. Rev. Lett. **16**, 797 (1966).